Biophysical Journal, Volume *122*

Supplemental information

Correlation between chemical denaturation and the unfolding energetics of *Acanthamoeba* actophorin

Nikhil Thota, Stephen Quirk, Yi Zhuang, Erica R. Stover, Raquel L. Lieberman, and Rigoberto Hernandez

Biophysical *Journal*
Supplementary Material

Supplementary Material for "Correlation Between Chemical Denaturation and the Unfolding Energetics of Acanthamoeba Actophorin"

Nikhil Thota[1], Stephen Quirk[2], Yi Zhuang[3], Erica R. Stover[3], Raquel L. Lieberman[4], and Rigoberto Hernandez[1,3,5,*]

[1]Department of Chemical and Biomolecular Engineering, Johns Hopkins University, Baltimore, MD 21218
[2]Kimberly-Clark Corporation, Atlanta, GA 30076-2199
[3]Department of Chemistry, Johns Hopkins University, Baltimore, MD 21218
[4]School of Chemistry and Biochemistry, Georgia Institute of Technology, Atlanta, GA 30332
[5]Department of Materials Science and Engineering, Johns Hopkins University, Baltimore, MD 21218
[*]Correspondence: r.hernandez@jhu.edu

CONTENTS

In this supplementary material, we report the potential of mean force (PMF) with work trajectories of unfolding the wild type and mutant Acto at 10 Å/ns pulling speed.

Figures S1, S2, and S3 illustrate the unfolding of Acto-2 it its periodic box in each of the 20 stages. Through the use of the telescoping box method, each of these stages has a different length along the z-axis shown here along the lateral direction. Specifically, the cross section of the periodic water box is fixed at 60 x 60 Å, and only the dimension of the box was increased along the z axis.

The PMF profiles and the underlying nonequilibrium trajectories are shown in Fig. S4. The Jarzynski weighted cumulative error over the ensemble of 100 nonequilibrium trajectories was determined at the end of each stage following the method in Ref. 1. These errors are listed in Table S1, and illustrated in Fig. S4.

For the wild type Acto, the standard deviation of the total work was about 1.716 kcal/mol, while it was 1.680 kcal/mol for Acto-2.

Figure S5 shows the fraction of residues that are retained in each of the secondary structures as the protein is unfolded along the trajectory closest to the Jarzynski Average. A notable region of interest lies between 160 and 200 Å Δr_{ee} where the fraction of α-helices retained in Acto-2 is higher than that compared to Acto-WT. This region coincides with the region in the plot of $\Delta\Delta U_{PMF}$ shown in Fig. S5A, and in which we see an increase in the work of unfolding the mutant.

Figure S6 shows the evolution of the different nonbonded interactions at sites 21 and 22 in Acto-WT and Acto-2 highlighted in Fig. 10 in the main text. The trends in these structures reflect those seen in the fraction of α helices in Fig. S5C. Specifically, at Δr_{ee} = 180Å, we see the α-helix breaking contact with the β-sheet as it starts to uncoil in Acto-WT, but it remains fairly intact in case of Acto-2. This is due to the ionic interactions introduced in Acto-2 by LYS 21 and LYS 22. Meanwhile, the α helix is anchored to the β strand in part because of the ionic interactions between LYS 21 with GLU 69 and ASP 67. In addition, the anchoring and rigidity of the α helix is also helped by the π-carbon interaction between LYS 22 with HSE 23, and the ionic and hydrophobic interactions between LYS 22 with GLU 16.

REFERENCES

1. Allen, C., H. R. Bureau, T. D. McGee, Jr., S. Quirk, and R. Hernandez, 2022. Benchmarking Adaptive Steered Molecular Dynamics (ASMD) on CHARMM Force Fields. *ChemPhysChem* 23:e202200175.

2. Humphrey, W., A. Dalke, and K. Schulten, 1996. VMD - Visual Molecular Dynamics. *J. Molec. Graphics* 14:33–38.

3. Stone, J., 1998. *An Efficient Library for Parallel Ray Tracing and Animation*. Master's thesis, Computer Science Department, University of Missouri-Rolla.

4. Frishman, D., and P. Argos, 1995. Knowledge-based protein secondary structure assignment. *Proteins* 23:566–579.

5. Jubb, J. C., A. P. Higueruelo, B. Ochoa-Montano, W. R. Pitt, D. B. Ascher, and T. L. Blundell, 2017. Arpeggio: A Web Server for Calculating and Visualizing Interatomic Interactions in Protein Structures. *J. Mol. Biol.* 429:365–371.

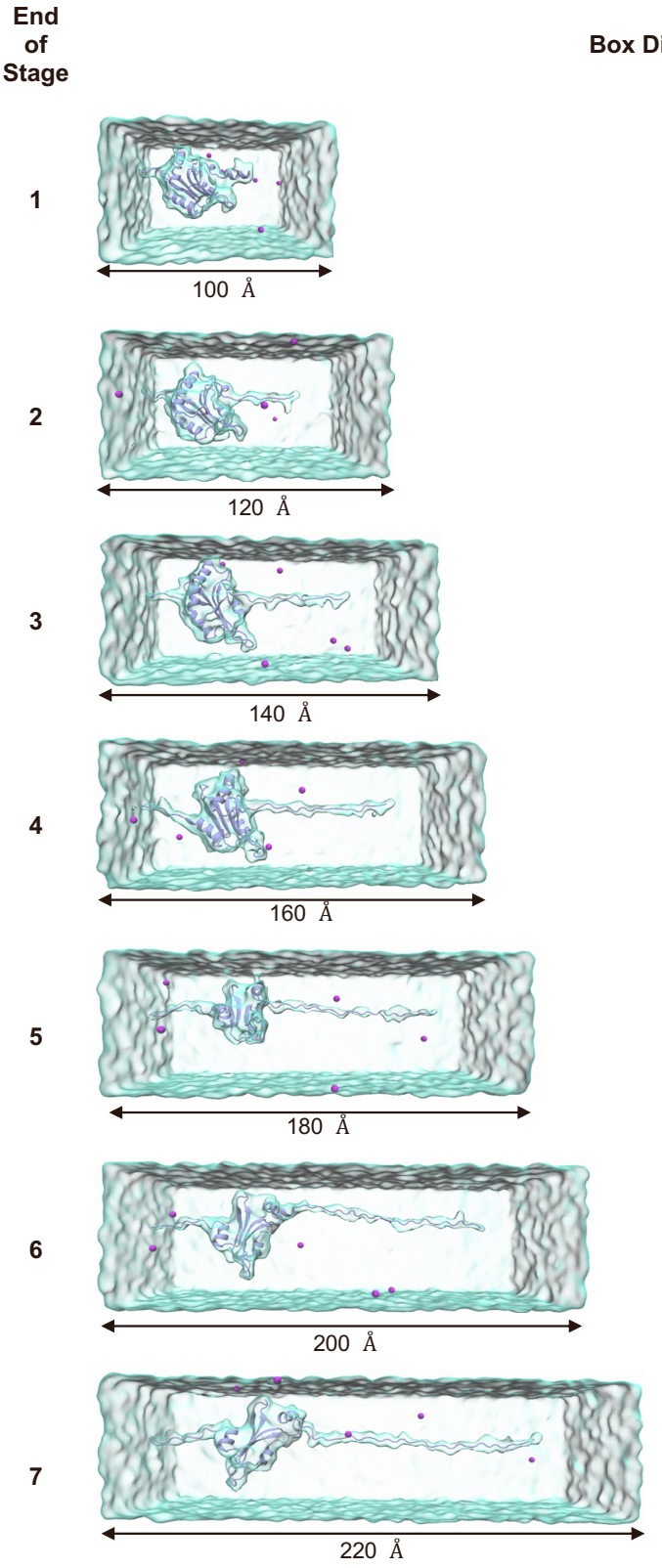

Figure S1: Representative boxes for Acto-2 in ice blue at the end of ASMD stages 1 through 7. Sodium ions are shown in purple. The cross section is 60Å × 60Å, and the length along the z-axis varies as indicated. Figures were created using the Tachyon plugin in VMD (2, 3).

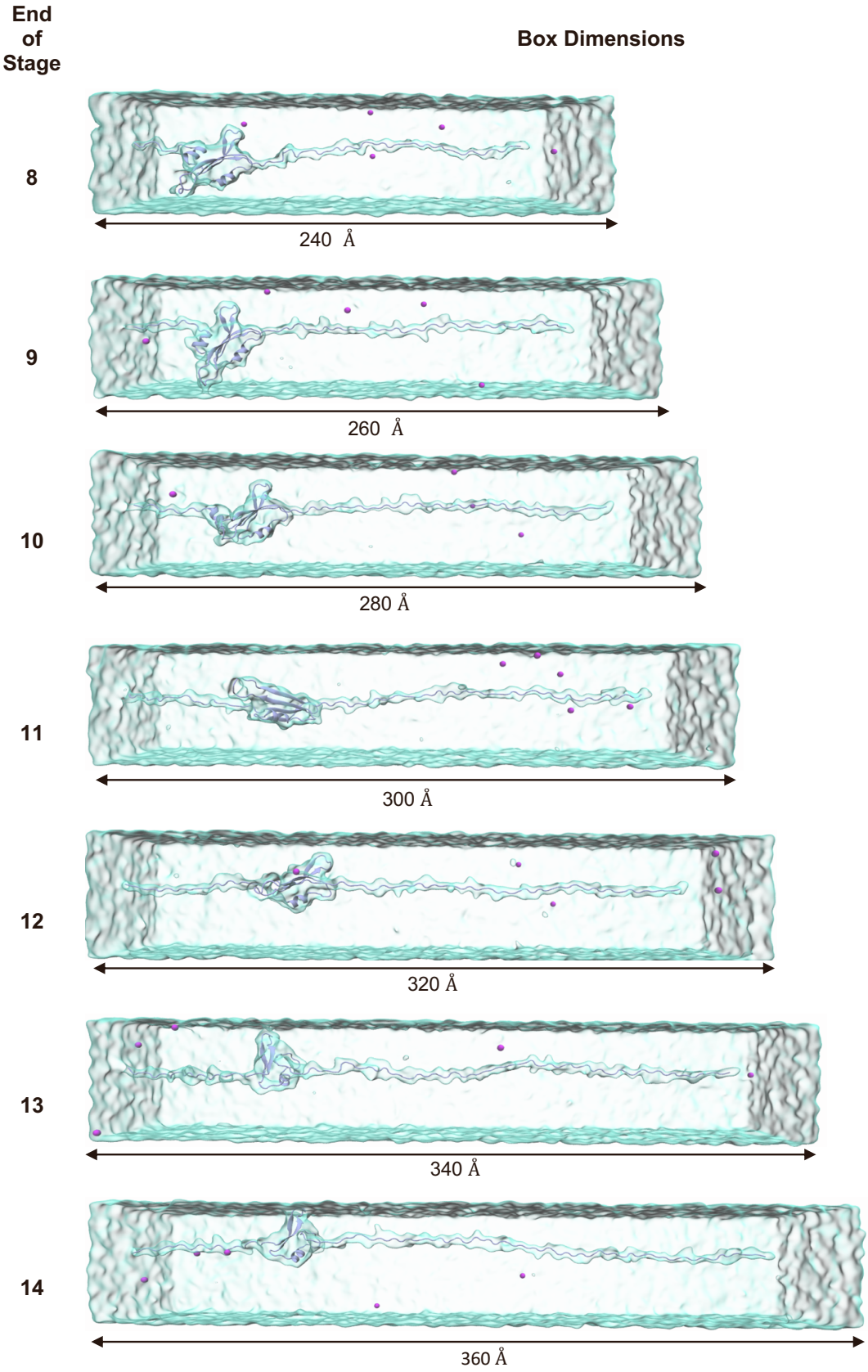

Figure S2: Representative boxes for Acto-2 in ice blue at the end of ASMD stages 8 through 14. All other descriptors are as in Fig. S1

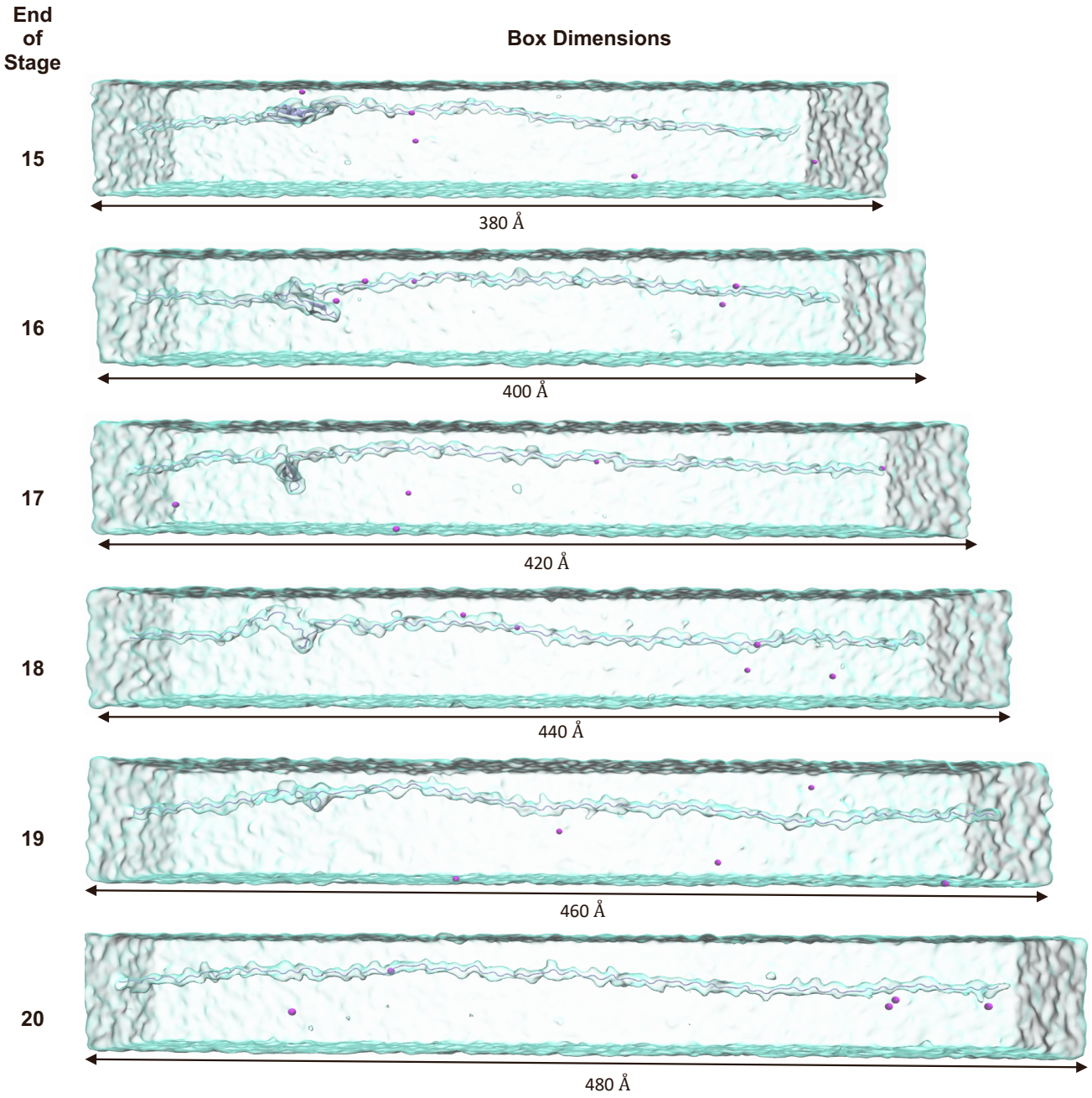

Figure S3: Representative boxes for Acto-2 in ice blue at the end of ASMD stages 15 through 20. All other descriptors are as in Fig. S1

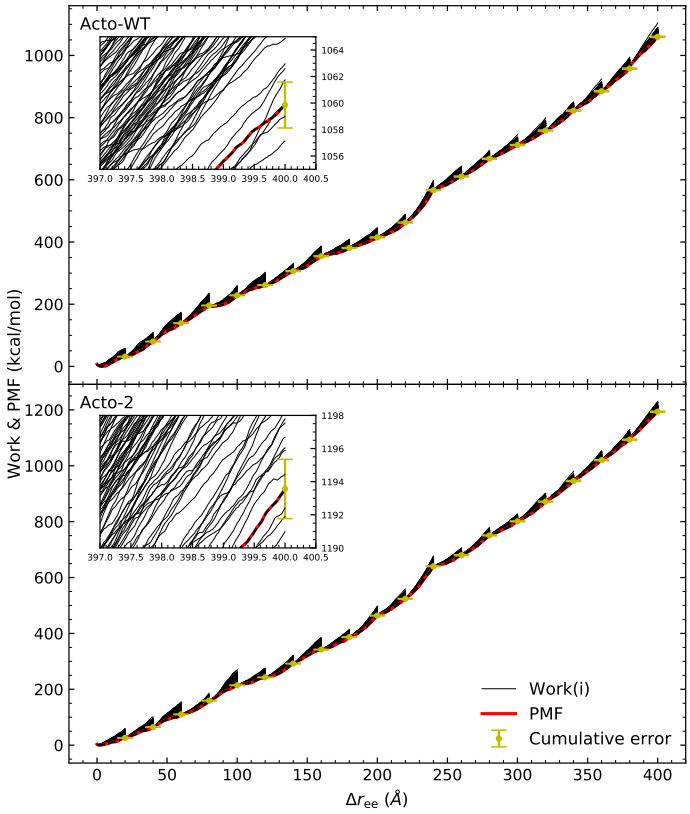

Figure S4: The work trajectories (black curves), PMF profiles (red curves) and error (yellow bars) were calculated for acto-WT (top) and acto-2 (bottom) using ASMD at 10 Å/ns pulling speed. The insets zoom-in to near the end of the last stages of the corresponding protein so as to illustrate the very small cumulative errors also listed in Table S1.

Table S1: The cumulative error at the end of each stage for both acto-WT and acto-2.

	acto-WT	acto-2
Stage	Cumulated Error (kcal/mol)	Cumulated Error (kcal/mol)
1	0.39346	0.03704
2	0.70846	0.04299
3	0.72928	0.28265
4	0.85334	0.72269
5	0.99001	0.72346
6	0.99086	0.72348
7	1.10918	0.83430
8	1.22148	0.83500
9	1.25491	0.98523
10	1.32139	1.12241
11	1.38987	1.15587
12	1.39819	1.15628
13	1.44122	1.30444
14	1.55749	1.37913
15	1.55964	1.42894
16	1.56715	1.55477
17	1.66400	1.60786
18	1.66872	1.70797
19	1.66874	1.71595
20	1.73154	1.78770

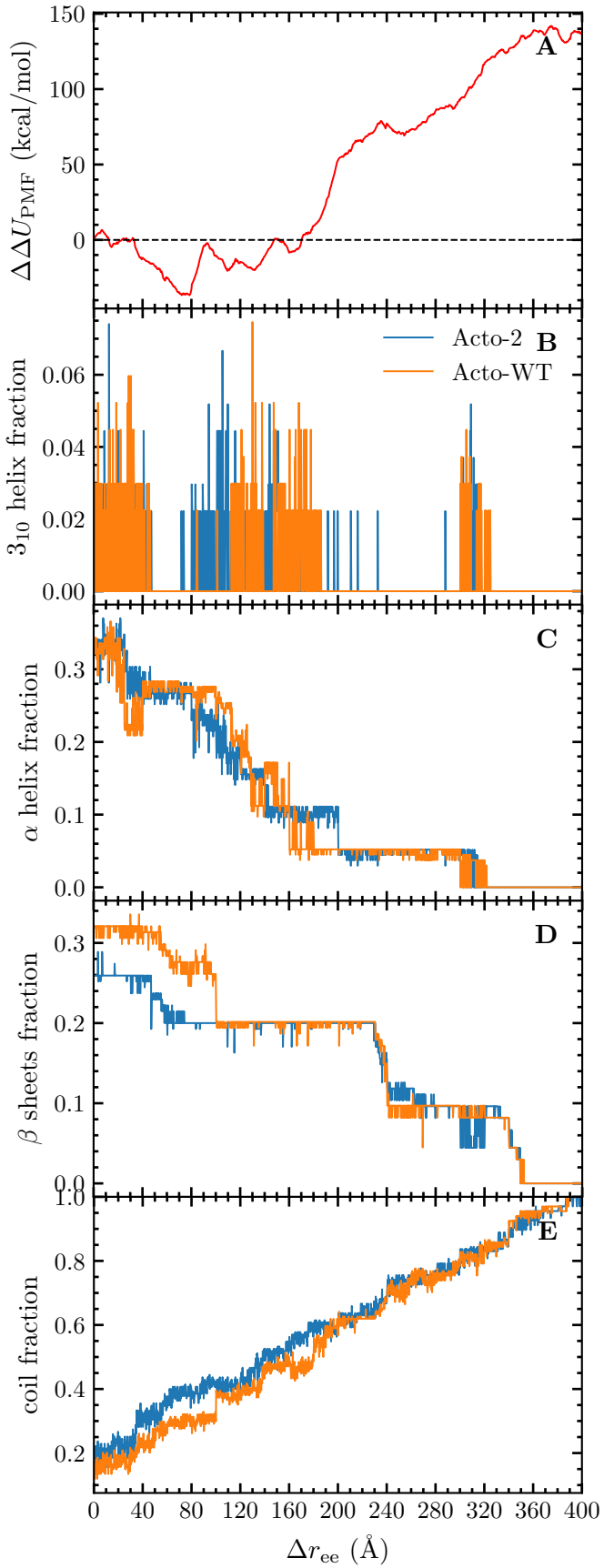

Figure S5: Energy and structural metrics along the JA trajectory of the Acto-2 (blue) and Acto-WT (orange) proteins: (A) The difference between the ΔU_{PMF} shown in Fig. S4 for the two proteins. (B) The fraction of 3_{10} helix secondary structure. (C) The fraction of α helix secondary structure. (D) The fraction of β helix secondary structure. (E) The fraction of residues in unfolded coil . The values were generated using the Timeline plugin in VMD (2, 4).

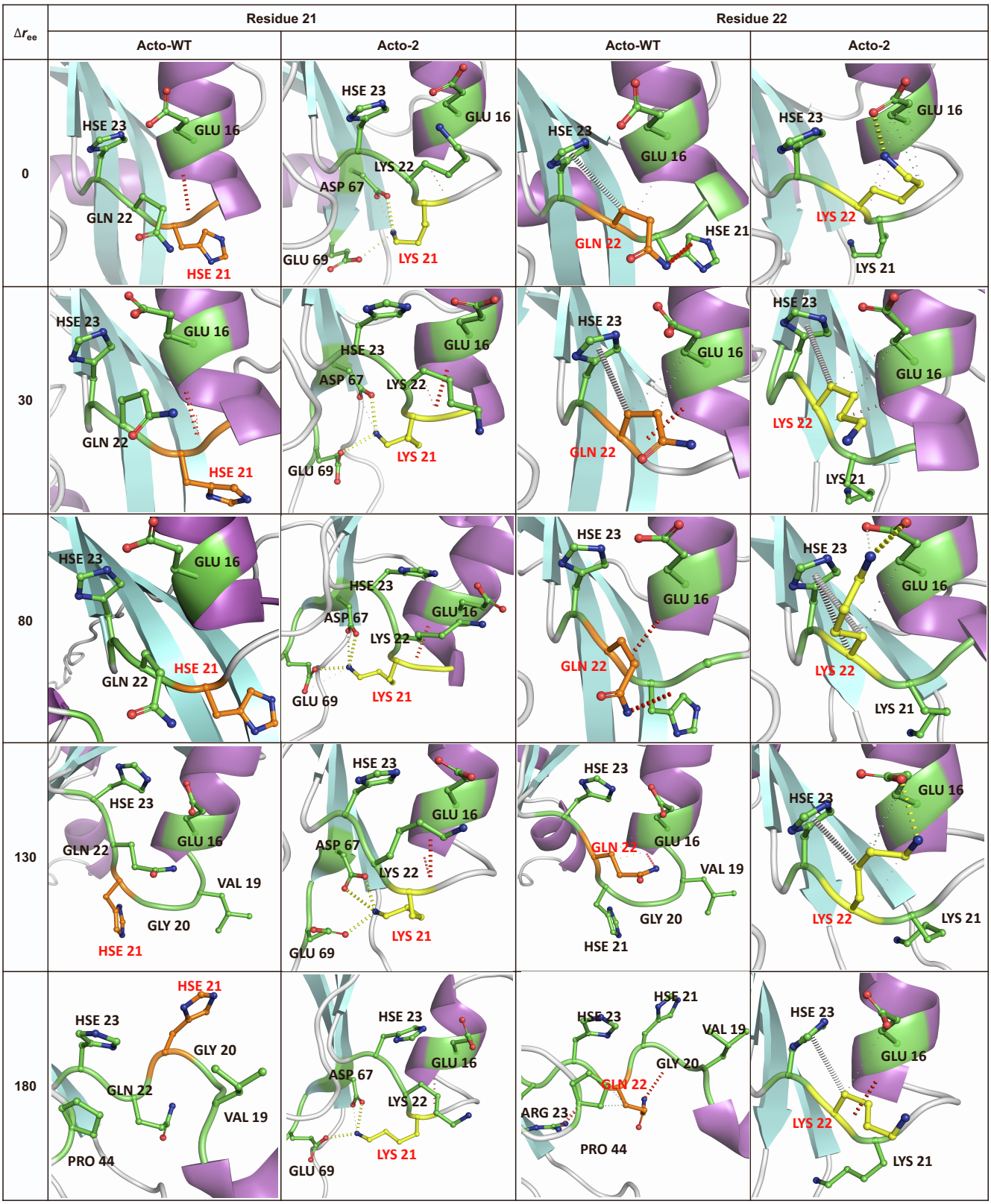

Figure S6: Ionic, hydrophobic and hydrogen bonding interactions at residues 21 and 22 for the Acto-WT and Acto-2 highlighted in Fig. 10 of the main paper, now shown at various points along the JA trajectory pulled through ASMD . Acto-WT residues at the noted sites are shown in orange while the corresponding mutations in Acto-2 are shown in yellow. The neighboring residues at each site are shown in green. Nonbonded interactions between residues are indicated by dotted lines. The type of nonbonded interaction is indicated by color and strength of interaction is indicated by the thickness of the dash. Hydrophobic interaction are indicted by green, hydrogen bonding interactions by red, salt bridge interactions by yellow and π-Carbon interactions by white. Thick dashes indicate overlapping van der Waal's radii while thin dashes indicate interactions that are beyond the van der Waal's overlap radius but within 5 Å. Nonbonded interactions were calculated using the Arpeggio web server (5) and visualizations were rendered using PyMol.